

## INFLUENCE OF ANTECEDENT PRECIPITATION ON SLOPE FAILURES AT THE YOKOGAKI-TOGE PASS

Yuko Ishida<sup>1</sup>, Tsuyoshi Kibayashi<sup>2</sup>, Tatsuo Konegawa<sup>3</sup>, Masamitsu Fujimoto<sup>2</sup> and Ryoichi Fukagawa<sup>2</sup>

<sup>1</sup>Institute of Disaster Mitigation for Urban Cultural Heritage, Ritsumeikan University, JAPAN,

<sup>2</sup>Department of Science and Engineering, Ritsumeikan University, JAPAN; <sup>3</sup> Mihama Town, JAPAN

**ABSTRACT:** The heritage of many cultures of the world consists of buildings, including shrines, temples, and ruins; only two such heritages have places of pilgrimage that incorporate roads. One of these is the Kumano pilgrimage route, along which there is a risk of sediment disasters. In 2011, Typhoon Talas caused collapses at Yokogaki-toge, which is part of the Kumano pilgrimage route. Two studies examining the localized characteristics of the rainfall, and how the rainfall contributed to slope failures at Yokogaki-toge, are described in this paper. Seepage flow analysis was carried out based on two types of rainfall, which enabled us to identify the characteristics of the rainfall event which triggered the collapse. Our results indicate that the characteristics of antecedent precipitation affect the infiltration characteristics, and the formation of a saturated zone. Localized rainfall was observed at multiple locations within Yokogaki-toge, with regional variations in the amount of rainfall. North-facing slopes are subjected to more rainfall than south-facing slopes, which may cause more weathering of these north-facing slopes.

*Keywords: Slope failure, Infiltration analysis, Rainfall characteristics, Risk Management of Cultural assets.*

### 1. INTRODUCTION

“Yokogaki-toge” is part of the world heritage site “Sacred Sites and Pilgrimage Routes in the Kii Mountain Range”. Since ancient times, the Kii Mountain Range has been considered in Japanese mythology to be a special place where gods dwell. This world heritage site, which is located on the Kii Peninsula in central Japan, consists of three sacred sites and pilgrimage routes. These routes are inseparable from the nature of the Kii Mountain Range. The roads that comprise this world heritage site are approximately 307.6 km long [1]; Yokogaki-toge is approximately 1.8 km long. Many people experience a feeling of spirituality, known as “Wabi-Sabi”, when travelling this beautiful route, shown in Photo 1. The route is approximately 1,200 years old.

The majority of the pilgrimage route is geologically vulnerable and slope failures often occur along its course. In Yokogaki-toge, a landslide occurred in the rainy season of 2007, and a deep-seated landslide, slope failure, and debris flow occurred in 2011 during Typhoon Talas, as shown in Photo 2. Mass movements such as landslides, slope failures, surface failures, and debris flows result from a combination of factors. Our study focused on rainfall as a trigger for slope failures. Little is known about the localized rainfall characteristics that occurred at the mountain side and their impact on slope failure. The aims of this study are to reveal how rainfall caused the collapse in 2011 and the characteristics of localized rainfall at Yokogaki-toge.



Photo. 1 The “Yokogaki-toge” Pilgrimage Route



Photo. 2 The deep-seated landslide at Yokogaki-toge

## 2. ANALYSIS AND EVALUATION OF FACTORS CAUSING COLLAPSE

Using suitable analysis method to understand a phenomenon of mass movement at the study region is important. Almandalawi et al, indicated the possible of rockfall risk assessment such as slope benches involved in the initiation of rockfalls, and the maximum run-out distance, using static general limit equilibrium methods and finite element stress analysis at open cut mining in Australia[2]. Sugawara investigated cause and countermeasure works of previous slope failures, and indicated suitable considerations in the Makinohara region which have many typical tea plantation[3]. Hytiris et al, measured the properties of the soil-root composite in laboratory, and evaluated their qualities for resisting landslide[4].

Different types of mass movement occurred at Yokogaki-toge, as shown in Fig.1. To predict the type and size of the collapses which can occur at Yokogaki-toge, we must understand the factors contributing to, and the mechanisms of, collapse. Geological factors such as the slope angle, aspect, and curvature were analyzed using geographical information systems (GIS), and the mechanisms causing collapses were estimated using field and document-based surveys. We identified the geological structure as the main cause of collapse.

### 2.1 The rainfall causing the collapses

To predict when collapse will occur, determining exactly which rainfall events have caused collapse is informative. We used two methods to measure this. One was AMeDAS, an automated meteorological data-acquisition system, which makes direct measurements in the field. The other was Rader-AMeDAS, which is obtained from radar observations and is corrected the observational error using AMeDAS data. The nearest AMeDAS point is approximately 3.5 km from Yokogaki-toge, and Rader-AMeDAS data is available on each point in a 1 km mesh. Seepage flow analysis was carried out using these two kinds of rainfall data including Typhoon Talas, with the intention of establishing the collapse conditions.

### 2.2 Localized characteristics of rainfall

Generally, large, deep landslides result from a high volume rainfall event with or without the high-intensity rainfall that can occur at the end of such an event. Surface failure results from high-intensity rainfall following a medium rainfall event. Since the characteristics of a rainfall event might enable us to predict the configuration and scale of

collapse, we focused on the following questions:

1. Is there a notable difference in rainfall characteristics at local sites?
2. Is the rainfall at a collapse site greater than the rainfall at a site which did not collapse?
3. Would a north-facing slope collapse because the amount of rainfall on it is greater than on a south-facing slope?

Since August 2014, nine rain gauges have been set up on Yokogaki-toge, as shown in Fig.1. Their configuration enables us to deduce the localized rainfall characteristics: Nos. 1 and 2 were on the south-facing slope; Nos. 3 and 4 were on the north-facing slope. The north and south slopes are approximately 100 m apart. Nos. 5–9 were placed 100–300 m apart on the east- and southeast-facing slopes. Nos. 1–4 were on the deep-seated landslide site; No. 6 was on the slope failure site; No. 7 was on the debris flow site; and Nos. 5, 8, and 9 were on slopes which did not collapse. Ideally, rain gauges should be set in unobstructed open space [5]; however, there are few such places in the site because of its forest. Consequently, gauge No. 1, and Nos. 4–9, were affected by shielding from trees. Nos. 2 and 3 were set in the relatively-open space caused by the collapse.

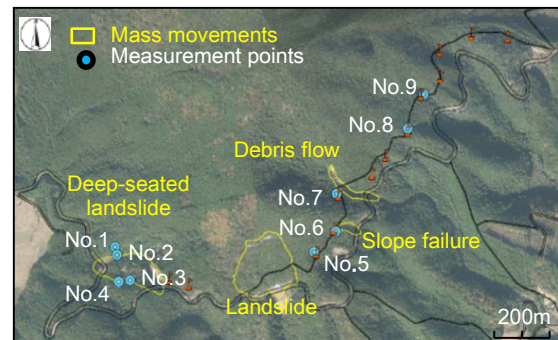


Fig.1 Measurement spots [6]

## 3. INFILTRATION ANALYSIS

### 3.1 Analysis condition

We used two types of rainfall data to deduce the characteristics of the rainfall event that caused the collapse in 2011: AMeDAS and Rader-AMeDAS. Figure 2 shows the two types of rainfall data, collected during the slope failure of 2011 [7]. Cases 1 to 8 in Fig. 2 indicate the time of evaluation. We performed saturated-unsaturated seepage flow analysis using PLAXIS 2D PlaxFlow (Plaxis; Delft, The Netherlands), which is a finite element analysis software package, to elucidate the differences between the two types of data. This software calculates seepage flow using Darcy's equation. The parameters were determined by performing experiments on soil samples and taking

values from the literature. Table 1 shows the hydraulic conductivity of each soil sample. The slope model shown in Fig. 3 was determined from a field survey and standard penetration tests, which were conducted in the landslide area.

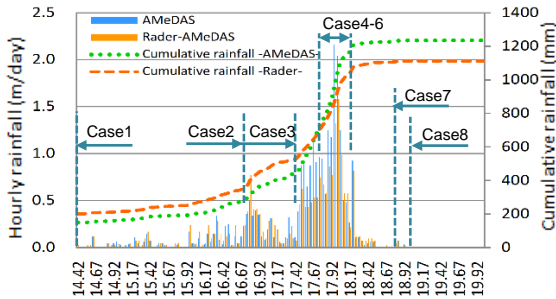


Fig. 2 Two kinds of rainfall data for the period from 17 August to 4 September, 2011

Table.1 Hydraulic conductivity of each soil

|                      | k: Hydraulic conductivity (m/s) |
|----------------------|---------------------------------|
| ① Colluvial soil     | $1.5 \times 10^{-4}$            |
| ② Weathered rhyolite | $1.5 \times 10^{-5}$            |
| ③ Talus sediment     | $4.6 \times 10^{-5}$            |
| ④ Weathered mudstone | $4.6 \times 10^{-6}$            |
| ⑤ Mudstone           | $1.0 \times 10^{-7}$            |
| ⑥ Embankment         | $1.0 \times 10^{-5}$            |

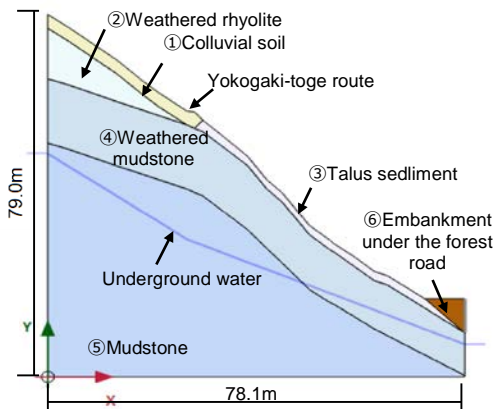


Fig. 3 Slope model

### 3.2 Analysis results

We started the analysis on 17<sup>th</sup> August 2011, 2 weeks before the rainfall event that caused the collapse. The collapse was estimated to have occurred on either September 3<sup>rd</sup> or 4<sup>th</sup>. Although hourly rainfall differed, as shown in Fig. 2, the times at which the rain started and stopped were very similar. The flow velocity conditions were evaluated for the 8 cases shown in Table 2. Table 3 summarizes the time of analysis and cumulative

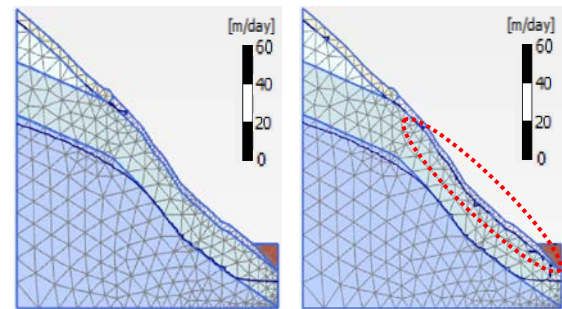
rainfall in each case. The flow velocity vector and phreatic line diagrams for each case are shown in Fig. 4. The diagram on the left is based on the measured AMeDAS rainfall, and the one on the right side uses the Rader-AMeDAS data.

Table.2 Cases and conditions

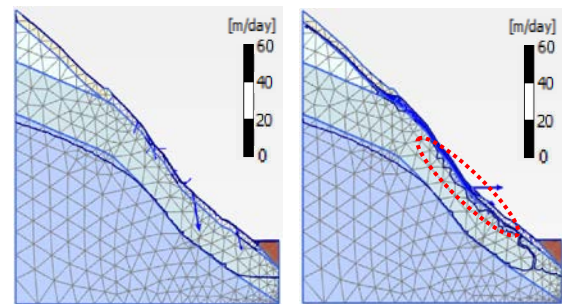
| Case | Conditions                                   |
|------|--|
| 1    | at the end of the antecedent precipitation   |
| 2    | at the end of a small rainfall event         |
| 3    | at the beginning of the large rainfall event |
| 4-6  | near the peak rainfall, including the peak   |
| 7    | 17 hours after the peak                      |
| 8    | 24 hours after the peak                      |

Table.3 Cumulative time and rainfall in each case

| Case | Time(day) | Cumulative rainfall |                  |
|------|-----------|---------------------|------------------|
|      |           | AMeDAS(mm)          | Rader-AMeDAS(mm) |
| 1    | 14.42     | 201                 | 151              |
| 2    | 16.71     | 355                 | 284              |
| 3    | 17.42     | 527                 | 444              |
| 4    | 17.83     | 755                 | 787              |
| 5    | 17.96     | 878                 | 978              |
| 6    | 18.00     | 944                 | 1063             |
| 7    | 18.71     | 1105                | 1226             |
| 8    | 20.00     | 1111                | 1235             |

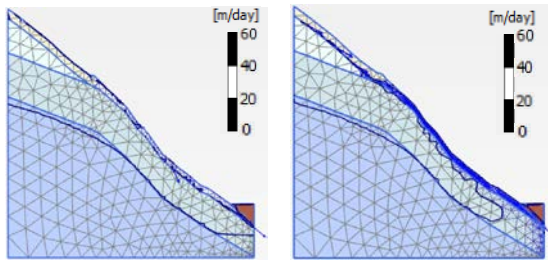


Case 1: At the end of the antecedent precipitation

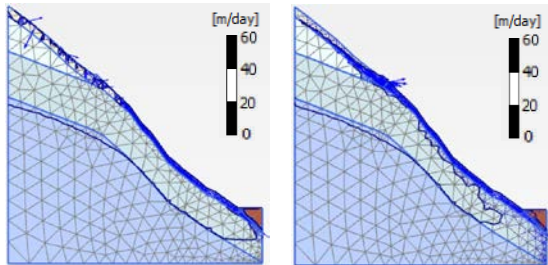


Case 2: At the end of the small rainfall

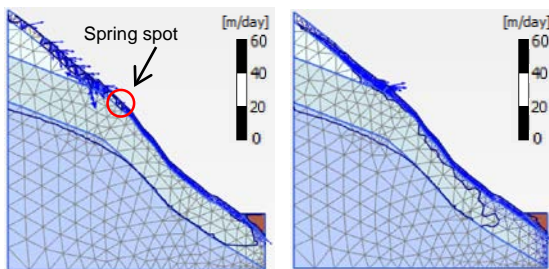
Fig.4 Flow velocity vector and phreatic lines



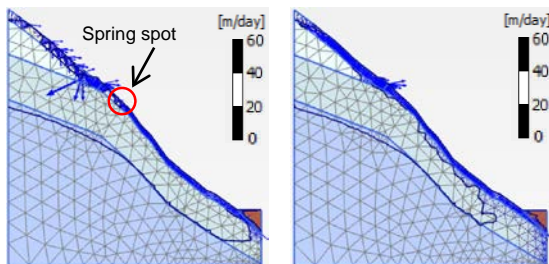
Case 3: At the beginning of the large rainfall



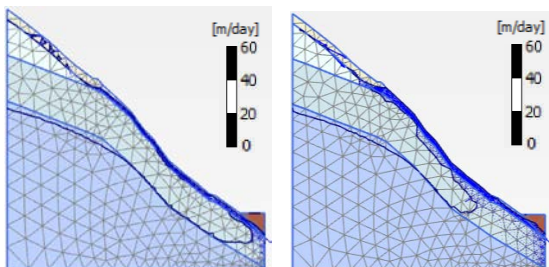
Case 4: Before the peak rainfall



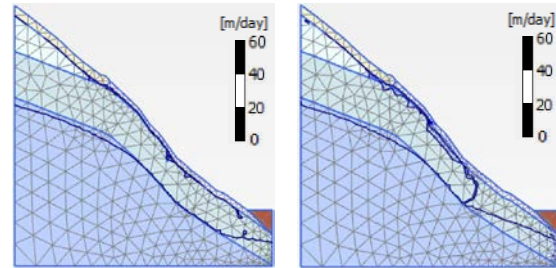
Case 5: Peak 1 (AMeDAS 90mm/h, Rader 55mm/h)



Case 6: Peak 2 (AMeDAS 85mm/h, Rader- AMeDAS 66mm /h)



Case 7: 17 hours after the Rader-AMeDAS peak



Case 8: 24 hours after the Rader-AMeDAS peak

Fig.4 Flow velocity vector and phreatic lines (continued)

The characteristics of the flow velocity vectors and phreatic lines in each figure are:

- Case 1: At the end of the antecedent precipitation
- Phreatic lines arose at the geological boundary between the talus sediment layer and the weathered mudstone layer, shown to the right (Rader-AMeDAS).
- Case 2: At the end of a low volume rainfall
- Downward-facing flow velocity vectors from the surface to the weathered mudstone layer are seen in the left figure (AMeDAS).
  - Many flow velocity vectors are seen in the surface layer, which is composed of talus sediment, shown in the right figure (Rader-AMeDAS).
  - The phreatic line in the mudstone layer is connected to the phreatic lines that developed on the upper side of the weathered mudstone layer toward the geological boundary in the right figure (Rader-AMeDAS).
- Case 3: At the beginning of the heavy rainfall
- Phreatic lines arose at the bottom of the talus sediment layer, shown in the left figure (AMeDAS).
  - The phreatic line formed in the saturated zone at the adjoining talus sediment, the weathered mudstone, and the mudstone layers. (Rader-AMeDAS).
- Case 4: Before the peak rainfall
- Many flow velocity vectors are found in the colluvial soil and talus sediment layers, shown in the left figure (AMeDAS).
  - Flow velocity vectors are concentrated at the geological boundary between the colluvial soil layer and the talus sediment layer, shown in the right figure (Rader-AMeDAS).
- Case 5: Peak 1
- Upward- and downward-facing flow velocity vectors are seen in the colluvial soil layer, and slight flow velocity vectors arose at the center of the slope near the spring, shown in the left figure (AMeDAS)

- Flow velocity vectors increased slightly in the colluvial soil layer, shown in the right figure (Rader-AMeDAS).

Case 6: Peak 2

- Flow velocity vectors increased at the boundary between the colluvial soil and the talus sediment layers, shown in the left figure (AMeDAS).
- Flow velocity vectors increased slightly in the colluvial soil layer, shown in the right figure (Rader-AMeDAS).

Case 7: 17 hours after the Rader-AMeDAS peak

- Flow velocity vectors and phreatic lines weakened on both slopes (AMeDAS, Rader-AMeDAS).

Case 8: 24 hours after the Rader-AMeDAS peak

- Many flow velocity vectors and phreatic lines disappeared on both slopes (AMeDAS, Rader-AMeDAS).

**3.3 Infiltration characteristics based on AMeDAS and Rader-AMeDAS**

In the case of AMeDAS, there were very few phreatic lines until the beginning of the heavy rainfall. Most of rainfall flowed past rather than forming a saturated zone at the surface layer. Before the peak of the heavy rainfall event, some phreatic lines arose at the bottom of the colluvial soil layer and at the top of the slope. However, these layers were not successive. Therefore, the directions of the flow velocity vectors in the colluvial soil were not uniform, and the vectors in the talus sediment layer were at similar angles to the layer. At the peak, upward-facing vectors arose on the middle slope near the spring. A saturated zone formed in the talus sediment layer, due to the rainfall, but did not spread to the deeper or upper layers.

In the case of the Rader-AMeDAS data, until the beginning of the heavy rainfall event, the cumulative rainfall is less than that measured by AMeDAS. Accumulated scanty rainfall caused many phreatic lines at the upper side of the weathered mudstone layer, and a saturated zone formed at the surface early into the rainfall. Near the peak, a large saturated zone formed at the surface layers, which were composed of colluvial soil and talus sediment. The angle of the flow velocity vectors in the colluvial soil and talus sediment layers were similar to those of the layer. The vectors near the geological boundary between the two surface layers were upward-facing.

The results from two kinds of rainfall indicate different infiltration characteristics. According to our results, the characteristics of antecedent precipitation caused the difference in infiltration characteristics, and affected the formation of the

saturated zone. In the neighboring saturated zone, the flow velocity vectors face in the same direction.

**4. CHARACTERISTICS OF MEASURED RAINFALL AT YOKOGAKI-TOGE**

Rainfall was observed at nine points at Yokogaki-Toge. The rain gauge No.1 had a loose connection during the 4-month measurement period. Therefore, the results were analyzed without data from this gauge. Figure 5 compares the rainfall data for the collapsed and non-collapsed sites. The AMeDAS data farthest to the left (green), called Mihama, were obtained by the Japan Meteorological Agency, and used as the standard rainfall [7]. The three right-most bars (blue) are from the non-collapsed site, and the other bars (red) show the rainfall at the collapsed site. The upper figure compares the total amount of rainfall; the middle figure compares the maximum hourly rainfall; and the lower figure compares the maximum rainfall over a 10-minute period. The shielding effect of the trees is seen in the total amount of rainfall and maximum hourly rainfall. Excluding sites Nos. 2 and 3, which were not shielded by trees, the total and maximum hourly rainfall at the collapsed site did not differ markedly from that at the non-collapsed sites.

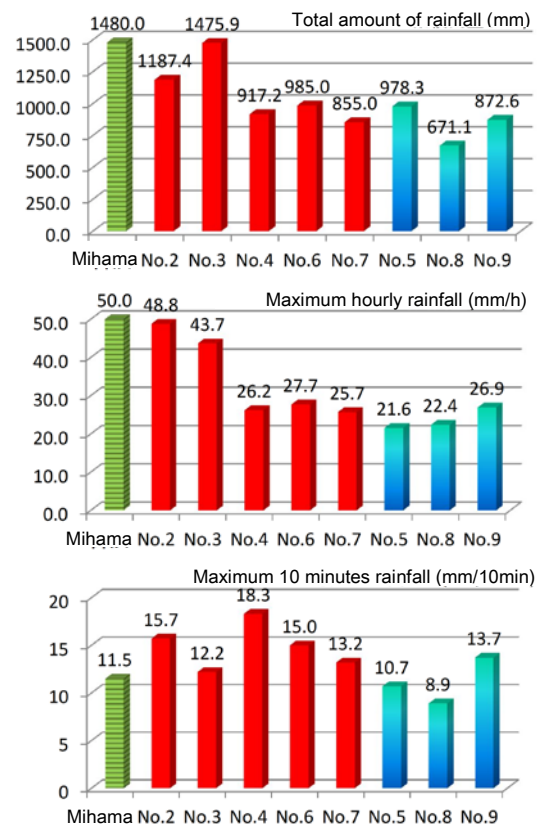


Fig. 5 Rainfall data for each rain gauge

However, the amount of rainfall at the collapsed site was slightly greater than that at the non-collapsed site. The maximum 10-minute rainfall differed by location regardless of whether the surface at that location collapsed.

Thirty rainfall events during the observation period were extracted using the following procedure: if the rain stopped for > 24 hours, a rainfall event was counted as a string of data. Rainfall events involving < 20 mm of cumulative rainfall were excluded. Figure 6 shows the directions of the slopes around Yokogaki-toge made from topographic data. The deep-seated landslide started from the tops of the north- and west-facing slopes.

To investigate the influence of rainfall on collapse, the data for No. 3 (north-facing slope) and No. 2 (south-facing slope) were compared, as shown in Fig 7. The red bars in Fig 7 show the differences in cumulative rainfall, calculated by subtracting the data for the south-facing slope from that of the north-facing slope. The blue points in Fig 7 show the cumulative rainfall of each rainfall event. Generally, the cumulative rainfall for each event was greater on the north-facing slope than on the south-facing slope. At first glance, this suggests that the collapsed slope and the slope receiving a large amount of rainfall are the same, and that there is a correlation between the cumulative rainfall during each event and the difference in rainfall between the north- and south-facing slopes. However, the trend differed for heavy rainfall events, which might trigger a collapse, as seen for events #13 and #15. In the case of events #13 and #15, which had over 100 mm cumulative rainfall, their difference was small, or more rainfall was measured on the south-facing slope than on the north-facing slope. Therefore, it is possible that the influence of the rate of rainfall on the risk of collapse is lower than that of other factors, such as the geological structure of the slope. The total amount of rainfall on the north-facing slope was greater than on the south-facing slope, which means weathering may be an indirect cause of collapse.



Fig. 6 Slope direction at Yokogaki-toge [8]

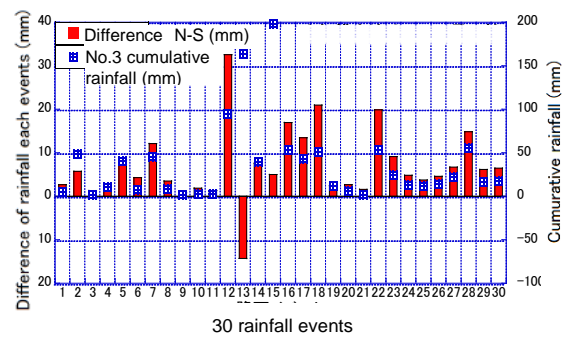


Fig. 7 Differences in rainfall (subtracting south-facing from north-facing)

## 5. CONCLUSION

We discussed the characteristics of the rainfall event that caused a slope to collapse in terms of infiltration analysis and multi-point rainfall measurements.

To predict collapse, knowing the volume and characteristics of the rainfall that caused the slope to collapse is important. We carried out infiltration analysis based on two types of rainfall data using a model of the slope before collapse. The seepage processes and the positions of the phreatic lines based on the two types of rainfall differed. In the case of the AMeDAS data, seepage occurred in the talus sediment layer, while analysis of the Rader-AMeDAS data indicated that phreatic lines were present in a broad area. We hypothesize that differences in antecedent precipitation caused the differences in the infiltration characteristics, and hence, the formation of saturated zones.

The characteristics of the rainfall data from the AMeDAS and Rader-AMeDAS differ with respect to the measured actual rainfall volume on the collapse site. We made multi-point rainfall measurements to measure the local characteristics of the rainfall at Yokogaki-toge.

The rainfall measurements at Yokogaki-toge indicate the following:

1. The measured values lacked precision due to the shielding effect of trees.
2. The characteristics of the rainfall at the collapsed and non-collapsed sites did not differ significantly.
3. The difference in the amount of high-intensity rainfall during a short time at each site was larger than the differences in the total and maximum hourly rainfall.
4. Rainfall has less influence on the occurrence of deep-seated landslides than other factors.
5. The north-facing slope may experience more weathering, due to greater total rainfall, than the south-facing slope.

## 6. ACKNOWLEDGEMENTS

This work was supported by a Grant-in-Aid for Scientific Research (C) No. 26350380 (2014–2016) from the Japan Society for the Promotion of Science. We would also like to thank Kumano Agriculture and Forestry Office for providing the geological investigation data.

## 7. REFERENCES

1. Oda Seitaro: The world heritage “Sacred Sites and Pilgrimage Routes in the Kii Mountain Range”-history and challenge-, ECPR, No.1, pp.24-30, 2010.(in Japanese)
2. Maged Almandalawi, Greg You, Peter Dahlhaus, Kim Dowling and Mohannad Sabry, Slope stability and rockfall hazard analysis in open pit zinc mine, *International Journal of GEOMATE*, Vol.8 (Sl.No.15), pp.1143-1150, 2015.
3. Jun Sugawara, Characteristics of slope failures in makinohara, Japan, *International Journal of GEOMATE*, Vol.5 (Sl.No.10), pp.717-722, 2013.
4. Nicholas Hytiris, Michael Fraser and Slobodan B. Mickovski, Enhancing slope

stability with vegetation, *International Journal of GEOMATE*, Vol.9 (Sl.No.18), pp. 1477-1482, 2015.

5. Yoshinori Tsukamoto: Forest hydrology, Bun-eido publication, p.217, 1998.
6. Mie Prefecture: aerial photo data of south part of Mie prefecture, 2012.
7. Japan Meteorological Agency: meteorological data, <http://www.data.jma.go.jp/obd/stats/etrn/index.php>, (2015.2access).
8. Geospatial Information Authority of Japan: Basement map information, <http://fgd.gsi.go.jp/download/>, (2012.2.12access).

---

*International Journal of GEOMATE, Oct., 2016, Vol. 11, Issue 26, pp.2626-2632.*

MS No. 5378 received on July 17, 2015 and reviewed under GEOMATE publication policies. Copyright © 2016, Int. J. of GEOMATE. All rights reserved, including the making of copies unless permission is obtained from the copyright proprietors. Pertinent discussion including authors' closure, if any, will be published in Oct. 2017 if the discussion is received by April 2017.

**Corresponding Author: Yuko Ishida**

---